

# CORE ADVANTAGE DECOMPOSITION FOR POLICY GRADIENTS IN MULTI-AGENT REINFORCEMENT LEARNING

006 **Anonymous authors**

007 Paper under double-blind review

## ABSTRACT

013 This work focuses on the credit assignment problem in cooperative multi-agent  
 014 reinforcement learning (MARL). Sharing the global advantage among agents of-  
 015 ten leads to insufficient policy optimization, as it fails to capture the coalitional  
 016 contributions of different agents. Existing methods mainly assign credits based on  
 017 individual counterfactual contributions, while overlooking the influence of coalitional  
 018 interactions. In this work, we revisit the policy update process from a coalitional  
 019 perspective and propose an advantage decomposition method guided by the  
 020 cooperative game-theoretic core solution. By evaluating marginal contributions of  
 021 all possible coalitions, our method ensures that strategically valuable coalitions re-  
 022 ceive stronger incentives during policy gradient updates. To reduce computational  
 023 overhead, we employ random coalition sampling to approximate the core solution  
 024 efficiently. Experiments on matrix games, differential games, and multi-agent col-  
 025 laboration benchmarks demonstrate that our method outperforms baselines. These  
 026 findings highlight the importance of coalition-level credit assignment and cooper-  
 027 ative games for advancing multi-agent learning.

## 1 INTRODUCTION

031 Cooperative Multi-Agent Reinforcement Learning (MARL) aims to train a group of agents to jointly  
 032 maximize a shared objective in a common environment (Panait & Luke, 2005). Such a paradigm has  
 033 shown great potential in a wide range of applications (Hu et al., 2023), including autonomous driving  
 034 platoons (Shalev-Shwartz et al., 2016), multi-robot systems (Busoniu et al., 2008), and large-scale  
 035 network control (Ma et al., 2024). A key challenge in MARL is how to effectively coordinate de-  
 036 centralization agents so that they can learn global strategies that maximize the global return (Oliehoek  
 037 et al., 2008; Lowe et al., 2017).

038 Recent advances in policy-gradient algorithms have significantly improved stability and scalabil-  
 039 ity in multi-agent learning. Among these, MAPPO (Yu et al., 2022), a multi-agent extension of  
 040 PPO (Schulman et al., 2017), has become a state-of-the-art baseline for cooperative MARL. Build-  
 041 ing upon this, HAPPO and HATRPO (Kuba et al., 2021; Zhong et al., 2023) introduced sequen-  
 042 tial agent-wise updates to further stabilize learning, achieving superior performance across various  
 043 benchmarks.

044 However, these methods typically share the same global advantage value across agents, which can  
 045 result in suboptimal updates. This is primarily due to the synchronous nature of policy updates,  
 046 where shared credit fails to distinguish individual contributions and may hinder cooperation. Such  
 047 issues are often attributed to the Relative Overgeneralization (RO) problem. To mitigate this, sev-  
 048 eral approaches have explored more refined credit assignment techniques. Value-based methods like  
 049 VDN (Sunehag et al., 2017) and QMIX (Rashid et al., 2018), QTRAN (Son et al., 2019), QPLEX  
 050 (Wang et al., 2020b) and policy-gradient methods like LICA (Zhou et al., 2020), COMA (Foer-  
 051 ster et al., 2018), VDAC (Su et al., 2021), and FACMAC (Peng et al., 2021) assign credit from an  
 052 individual perspective and have improved coordination efficiency (Wang et al., 2022b; 2020c). Ad-  
 053 ditionally, DOP (Wang et al., 2020d) has tackled the exploration challenge from a maximum entropy  
 perspective.

Despite their success, these methods focus exclusively on either global or individual perspectives. Between these extremes lies an underexplored middle ground: coalitional granularity, where credits are evaluated and allocated at the level of agent subsets (i.e., coalitions  $C \subseteq N$ ). To address this gap, recent works have introduced Shapley value-based credit assignment from cooperative game theory into policy gradient methods (Wang et al., 2020a; Li et al., 2021; Wang et al., 2022a). While these approaches provide theoretically grounded individual attributions, they often lack interpretability in the context of multi-agent policy updates and rely on rigid baselines (e.g., no-op or zero actions), which reduce flexibility. Furthermore, many other meaningful cooperative game solutions remain unexplored in MARL.

In this paper, we propose **Core Advantage Decomposition (CORA)**, a novel credit assignment framework for multi-agent policy gradient methods. CORA estimates *coalitional advantages* by evaluating the marginal contributions of coalitions to the global return and decomposes credit using the *core solution* from cooperative game theory. This ensures *coalitional rationality* and preserves beneficial exploratory behaviors. To improve scalability, CORA employs *random coalition sampling* for efficient approximation.

The main contributions of this paper are threefold:

- Coalition-level credit assignment. We propose a novel coalitional advantage formulation and allocate credits via the strong  $\epsilon$ -Core, ensuring both global consistency and coalition rationality.
- Theoretical guarantees. We provide policy-improvement lower bounds at the coalition level, showing that CORA systematically reinforces beneficial coalitions. The coalitions with high potential advantage values will receive higher advantage values to promote collaborative strategy optimization.
- Practical effectiveness. We develop an efficient sampling approximation and demonstrate consistent performance gains across diverse MARL benchmarks, including matrix games, differential games, VMAS, SMAC, Google Research Football, and Multi-Agent MuJoCo.

## 2 RELATED WORK

This section provides an overview of key research areas relevant to our work, including traditional value decomposition methods, policy gradient methods.

### 2.1 VALUE DECOMPOSITION METHODS

Value decomposition methods aim to decompose the global value function in MARL into individual contributions from each agent, thereby facilitating decentralized learning. Value-Decomposition Networks (VDN) (Sunehag et al., 2017) is a pioneering approach that splits the joint action-value function into simpler, agent-specific value functions. This decomposition significantly reduces the complexity of multi-agent learning and allows for decentralized execution. QMIX (Rashid et al., 2018), an extension of VDN, introduces a monotonic mixing function that ensures the global Q-value is a monotonic combination of individual agent Q-values.

### 2.2 MULTI-AGENT POLICY GRADIENT METHODS

Policy gradient methods, particularly MAPPO (Multi-Agent Proximal Policy Optimization) (Yu et al., 2022), have become the dominant paradigm in MARL. MAPPO has shown significant performance improvements over earlier methods, such as COMA (Counterfactual Multi-Agent Policy Gradients) (Foerster et al., 2018) and MADDPG (Multi-Agent Deep Deterministic Policy Gradient) (Lowe et al., 2017). Attention-based credit assignment methods such as ATA (She et al., 2022) and spatiotemporal decomposition approaches such as STAS (Chen et al., 2024) improve multi-agent coordination by learning expressive representations of agent-time or space-time interactions. In contrast, our method formulates advantage decomposition as an  $\epsilon$ -core problem, ensuring that the allocated per-agent advantages satisfy coalition constraints for all sampled coalitions. Thus, CORA provides a complementary perspective: rather than learning a decomposition implicitly, it enforces a principled game-theoretic structure that guarantees consistency across coalitions.

108 2.3 CREDIT ASSIGNMENT BASED ON SHAPLEY VALUE  
109

110 Shapley-based methods in MARL, integrating cooperative game theory, address the credit assignment  
111 problem by fairly distributing rewards based on each agent’s contribution. Early work, such  
112 as SQDDPG (Wang et al., 2020a), uses the Shapley value in Q-learning and DDPG for continuous  
113 action spaces to calculate each agent’s marginal contribution.

114 A more recent advancement, Shapley Counterfactual Credit Assignment (SCCA) (Li et al., 2021),  
115 refines credit assignment by considering counterfactual scenarios, improving accuracy and stability.  
116 However, SCCA faces computational challenges in multi-agent settings. SHAQ-learning (Wang  
117 et al., 2022a) also integrates Shapley values into Q-learning, enhancing stability and fairness in  
118 cooperative tasks, but it struggles with scalability and efficiency.  
119

120 2.4 COOPERATIVE GAME THEORY AND THE CORE  
121

122 Cooperative game theory, traditionally used in economics (Driessen, 2013), is also applied in MARL  
123 for credit assignment. Recent works (Jia et al., 2019), (Ghorbani & Zou, 2019), and (Sim et al., 2020)  
124 have adopted the Shapley value for data valuation and reward allocation. In federated learning,  
125 (Chaudhury et al., 2022) and (Donahue & Kleinberg, 2021) applied cooperative game theory to  
126 fairness and stability.

127 The core (Driessen, 2013), another key concept in cooperative game theory, guarantees stability by  
128 ensuring no coalition of agents can improve their outcome by deviating from the allocation. While  
129 the Shapley value has been used for fair reward distribution in MARL, traditional methods often rely  
130 on a fixed baseline, limiting their applicability in dynamic environments. Additionally, they do not  
131 address interference from high-risk explorations in cooperative MARL.  
132

133 3 BACKGROUND  
134

135 This section provides an overview of the foundational concepts and challenges in MARL, focusing  
136 on policy gradient methods and the credit assignment methods.  
137

138 3.1 PROBLEM FORMULATION  
139

140 In cooperative multi-agent reinforcement learning, a group of agents works together to maximize  
141 a shared return within a common environment (Panait & Luke, 2005; Kuba et al., 2021). This  
142 setting can be formalized as a Markov game (Littman, 1994; Kuba et al., 2021; Zhao et al., 2024)  
143 defined by the tuple  $\mathcal{G} = \langle N, S, A, \mathbb{P}, r, \gamma \rangle$ , where  $N = \{1, \dots, n\}$  is the set of agents,  $S$  is the  
144 state space,  $A = \prod_{i \in N} A_i$  is the joint action space, with  $A_i$  being the action space of agent  $i$ ,  
145  $\mathbb{P} : S \times A \times S \rightarrow [0, 1]$  is the transition function,  $r : S \times A \rightarrow \mathbb{R}$  is the reward function, and  
146  $\gamma \in [0, 1]$  is the discount factor. At each time  $t \in \mathbb{N}$ , each agent  $i$  observes the full state  $s^t$ , and  
147 selects an action  $a_i^t \in A_i$  drawn from its policy  $\pi_i(\cdot | s^t)$ . The joint action  $a^t = (a_1^t, \dots, a_n^t)$  leads to  
148 the next state  $s^{t+1} \sim \mathbb{P}(s^{t+1} | s^t, a^t)$  and generates a common reward  $r^t = r(s^t, a^t)$  for all agents.  
149 The agents aim to update their policies that maximize the shared expected cumulative reward:  
150

$$151 \max_{\pi} J(\pi) = \mathbb{E}_{s, a \sim \pi, \mathbb{P}} \left[ \sum_{t=0}^{\infty} \gamma^t r(s_t, a_t) \right]. \quad (1)$$

154 Under the centralized training with decentralized execution (CTDE) paradigm Oliehoek et al.  
155 (2008); Lowe et al. (2017); Yu et al. (2022), each agent  $i$  is trained with global information and  
156 execute using only local observation  $o_i = O_i(s) \in \mathcal{O}_i$ . A central component in training pro-  
157 cess is the global state value function  $V(s)$  (the global state-action value function  $Q(s, a)$ ), es-  
158 timating the expected return from state  $s$  (after taking joint action  $a$ ). Denoting the advantage  
159  $A(s^t, a^t) = Q(s^t, a^t) - V(s^t)$  with GAE estimator

$$160 \quad 161 \quad A_{GAE}^t = \sum_{l=0}^{\infty} (\gamma \lambda)^l \delta_{t+l} \quad (2)$$

162 where  $\delta_t$  denotes the TD error  $\delta_t = r_t + \gamma V(s_{t+1}) - V(s_t)$ , a standard multi-agent policy gradient  
163 for agent  $i$  is

$$164 \quad \nabla_{\phi_i} J = \mathbb{E} [\nabla_{\phi_i} \log \pi_i(a_i|s) A_i(s, a)], \quad (3)$$

165 where individual advantage  $A_i(s, a)$  is the per-agent credit signal. Sharing the same advantage  
166  $A(s, a)$  across agents is simple and stable, but it fails to capture heterogeneous contributions of  
167 different agents, leading to inefficient credit assignment and slower convergence.

168 Throughout this paper, we focus on multi-agent credit assignment via advantage decomposition  
169 for policy-gradient methods, using it to drive policy updates that strengthen effective coalitional  
170 collaboration.

### 172 3.2 SHARING ADVANTAGE

174 Many credit assignment methods such as COMA Foerster et al. (2018), VDN Sunehag et al. (2017),  
175 QMIX Rashid et al. (2018), and LICA Zhou et al. (2020) assign advantage or value from individual  
176 or marginal perspective. In this paper, besides the global advantage, we also consider the coalitional  
177 advantage for each coalition of agents. Let  $N = \{1, \dots, n\}$  denote the set of all agents. For a given  
178 sample  $(s, a)$  where  $s = (s_1, \dots, s_n)$  and  $a = (a_1, \dots, a_n)$ , we evaluate the scenario where agents  
179 in coalition  $C \subseteq N$  take actions  $a_C$ , while each agent  $i \notin C$  execute a baseline action  $\bar{a}_i$  or current  
180 policy  $\pi_{N \setminus C}$ .

181 Sharing the global advantage  $A(s, a)$  among agents often leads to insufficient policy updates. This  
182 method incentivizes each agent to update its policy  $\pi_i(a_i|s_i)$  to either approach action  $a_i$  with  
183  $A(s, a) > 0$  or avoid those with  $A(s, a) < 0$ . Specifically, when an action  $a$  with  $Q(s, a) < V(s)$  is  
184 explored during training, all agents are penalized via  $A(s, a) < 0$ , and the policy  $\pi_i(a_i|s_i)$  for each  
185 agent is updated to reduce its probability. This occurs even if a coalition  $C$  could form a superior  
186 joint action  $(a_C, a'_{N \setminus C})$  satisfying  $Q(s, a_C, a'_{N \setminus C}) > V(s)$ .

187 Moreover, consider the case where the executed action  $a^*$  is already optimal. If agents in coalition  
188  $C$  explore a new action  $a_C$  while others act optimally, and  $Q(s, a_C, a^*_{N \setminus C}) < V(s)$ , then the prob-  
189 ability  $\pi_i(a^*_i|s_i)$  for each agent  $i \notin C$  is reduced due to  $A(s, a) < 0$ , destabilizing the probability  
190 distribution over the optimal action  $a^*$ .

191 In summary, the value of coalition actions can be further exploited. Agents with greater  
192 potential, such as those belonging to a coalition  $C$  where  $Q(s, a_C, \bar{a}_{N \setminus C}) \ll V(s)$  or  
193  $\mathbb{E}_{a_{N \setminus C} \sim \pi_{N \setminus C}} [Q(s, a_C, a_{N \setminus C})] \ll V(s)$ , should receive larger advantage values to encourage the  
194 action  $(a_C, \bar{a}_{N \setminus C})$ .

## 196 4 CORE ADVANTAGE DECOMPOSITION FOR MULTI-AGENT POLICY 197 GRADIENTS

200 In this section, we evaluate the advantage of coalition actions and propose an advantage decompo-  
201 sition algorithm.

### 203 4.1 COALITIONAL ADVANTAGE

205 Consider a global value function  $Q(s, a)$ , which describes the return of the joint action  $a$  in state  $s$ .  
206 The advantage of coalition  $C$ , denoted as  $A_C(s, a_C)$ , is defined as:

$$207 \quad A_C(s, a_C) = \mathbb{E}_{a_{N \setminus C} \sim \pi_{N \setminus C}} [Q(s, a_C, a_{N \setminus C})] - V(s), \quad (4)$$

208 where the first term  $\mathbb{E}_{a_{N \setminus C} \sim \pi_{N \setminus C}} [Q(s, a_C, a_{N \setminus C})]$  represents the expected return when coalition  
209  $C$  takes the sampled action  $a_C$ , and the other agents  $i \notin C$  follow the current strategy  $\pi_{N \setminus C}$ .  
210 Subtracting the baseline value  $V(s)$  gives the advantage of coalition  $C$  taking action  $a_C$  alone.  
211 Incidentally, the global value naturally satisfies  $A_N(s, a) = Q(s, a) - V(s) = A(s, a)$ . By defining  
212 the advantage in this way, we can clearly quantify the contribution of each coalition action  $a_C$  to the  
213 team.

214 Besides the definition  $A_C(s, a_C)$ , we can also consider defining it as:

$$215 \quad A_C(s, a_C) = Q(s, a_C, \bar{a}_{N \setminus C}) - V(s) \quad (5)$$

216 where  $\bar{a}_i$  represents a baseline action. The baseline action  $\bar{a}$  provides a reference for evaluating  
 217 coalition values. In our experiments, we mainly consider the most probable action as the baseline  
 218 action. This is because, regardless of whether a discrete softmax policy or a continuous Gaussian  
 219 policy is used, the most probable action is typically chosen during evaluation or execution. During  
 220 **training, however, actions are sampled from the probability distribution to encourage exploration.**  
 221 Specifically: (i) For discrete actions:  $\bar{a}_i = \arg \max_{a_i} \pi_{\theta_i}(a_i | s_i)$ , while training samples are drawn  
 222 from  $\pi_i(\cdot | s_i)$ ; (ii) For continuous actions:  $\bar{a}_i = \mu_{\theta_i}(s_i)$ . For example, a Gaussian policy outputs  
 223  $(\mu_i, \sigma_i)$ , with training samples  $a_i \sim \mathcal{N}(\mu_i, \sigma_i)$ , while the baseline action uses  $\mu_{\theta_i}(s_i)$ .

## 224 4.2 ADVANTAGE DECOMPOSITION

225 The next problem we need to solve is how to allocate advantage  $A_i(s, a)$  to each agent  $i \in N$  based  
 226 on  $2^n$  advantage values  $A_C(s, a_C)$  (for each  $C \subseteq N$ ). Intuitively, if a coalition action  $a_C$  yields a  
 227 high advantage value  $A_C(s, a_C)$ , the total advantage assigned to the agents in that coalition should  
 228 not be too small. Formally, we require

$$229 \sum_{i \in C} A_i(s, a) \geq A_C(s, a_C) - \epsilon. \quad (6)$$

230 This allocation principle aligns with coalitional rationality in cooperative game theory. If coalition  
 231 actions  $(a_C, \pi_{N \setminus C})$  are promising, it is beneficial to incentivize each  $a_i$  ( $i \in C$ ) to adjust its policy  
 232 distribution, thereby encouraging exploration of this action in the future.

233 Additionally, it is essential to ensure that  $\sum_{i \in N} A_i(s, a) = A_N(s, a) = A(s, a)$ , which is known  
 234 as effectiveness in cooperative game theory and is also widely adopted as a guiding principle in  
 235 value decomposition methods. For convenience, given current state  $s$  and action  $a$ , we denote the  
 236 advantage value of agent  $i$ ,  $A_i(s, a)$ , simply as  $A_i$ .

237 This form coincides with the classic solution Strong  $\epsilon$ -Core of cooperative game theory Driessen  
 238 (2013):

$$239 \text{Core}_\epsilon(N, A_C) = \left\{ (A_1, \dots, A_n) \in \mathbb{R}^n \mid \sum_{i \in N} A_i = A_N(s, a), \right. \\ 240 \left. \sum_{i \in C} A_i \geq A_C(s, a_C) - \epsilon, \text{ for } \forall C \subseteq N \right\}, \quad (7)$$

241 where  $\epsilon \geq 0$  is a non-negative parameter that allows for a small deviation from the ideal condition.

242 Generally, the  $\epsilon$ -core may admit infinitely many solutions, but not all of them are desirable. In  
 243 particular, some allocations satisfying coalition rationality may place all credit on a single agent,  
 244 leaving others without effective incentives. To avoid such imbalanced solutions, we introduce an  
 245 additional objective that penalizes large deviations from the uniform allocation. Specifically, we  
 246 minimize the variance of credits among agents, leading to the quadratic program:

$$247 \underset{\epsilon \geq 0, A_1, \dots, A_n}{\text{minimize}} \quad \epsilon + \lambda \sum_{i \in N} \left( A_i - \frac{1}{|N|} A_N(s, a) \right)^2, \\ 248 \text{subject to: } \sum_{i \in N} A_i = A_N(s, a), \\ 249 \sum_{i \in C} A_i \geq A_C(s, a_C) - \epsilon, \forall C \subseteq N. \quad (8)$$

250 This formulation ensures a more balanced allocation while respecting coalition rationality. In  
 251 detail,  $\mathbb{E}_{a_{N \setminus C}}[Q(s, a)]$  can be estimated using Monte Carlo sampling, approximately given by  
 252  $\frac{1}{|K|} \sum_{k \in K} Q(s, a_C, a_{N \setminus C}^k)$  where  $K$  is the set of sampled trajectories, and  $a_{N \setminus C}^k$  represents the ac-  
 253 tion taken by the agents in  $N \setminus C$  during the  $k$ -th trajectory. The diagram and pseudocode are shown  
 254 as Figure 7 and Algorithm 1. In summary, our framework requires two critics,  $Q(s, a)$  and  $V(s)$ ,  
 255 both updated using temporal-difference (TD) errors. The value critic  $V$  is employed for generalized  
 256 advantage estimation (GAE), which stabilizes policy updates; in addition, the global advantage (for  
 257 grand coalition  $N$ )  $A_N(s, a)$  is also estimated based on GAE. The state-action value critic  $Q$ , on the  
 258 other hand, is responsible for allocating the advantage  $A_i$ .

270 

## 5 THEORETICAL ANALYSIS

271  
272 In this section, we provide some theoretical analysis and approximate methods based on the designed  
273 CORA advantage value.274 **Theorem 1.** *Under compatible approximation and a natural policy gradient (NPG) step, for small  
275 step size  $\alpha > 0$ ,*

276  
277 
$$\Delta \log \pi_i(a_i | s) \approx \alpha A_i,$$
  
278  
279 
$$\Delta \log \pi(a | s) = \sum_{i=1}^n \Delta \log \pi_i(a_i | s) \approx \alpha A_N,$$
  
280  
281  
282 
$$\Delta \log \pi_C(a_C | s) = \sum_{i \in C} \Delta \log \pi_i(a_i | s) \approx \alpha \sum_{i \in C} A_i.$$

283  
284 **Theorem 2.** *Consider one NPG step  $\phi'_i = \phi_i + \alpha F_i^{-1} g_i$  with  $g_i := \mathbb{E}[\psi_i A_i]$ ,  $\psi_i := \nabla_{\phi_i} \log \pi_i(a_i | s)$ ,  $F_i := \mathbb{E}[\psi_i \psi_i^\top]$ , and step size  $\alpha > 0$ . Assume for each agent  $i$  that  $\log \pi_i(\cdot | s; \phi_i)$  is twice  
285 continuously differentiable and its Hessian is uniformly bounded on the line segment between  $\phi_i$   
286 and  $\phi'_i$ :*

287  
288 
$$\|\nabla_{\phi_i}^2 \log \pi_i(a_i | s; \xi_i)\|_{\text{op}} \leq L_i \quad \text{for all } \xi_i \in [\phi_i, \phi'_i].$$

289 Then for any coalition  $C \subseteq N$  and any sampled  $(s, a)$ ,

290  
291 
$$\Delta \log \pi_C(a_C | s) \geq \alpha \sum_{i \in C} A_i - \frac{\alpha^2}{2} \sum_{i \in C} L_i \|F_i^{-1} g_i\|_2^2. \quad (9)$$
  
292

293 If, in addition, the strong  $\epsilon$ -Core constraints hold,  $\sum_{i \in C} A_i \geq A_C(s, a_C) - \epsilon$ , then

294  
295 
$$\Delta \log \pi_C(a_C | s) \geq \alpha (A_C(s, a_C) - \epsilon) - \frac{\alpha^2}{2} \sum_{i \in C} L_i \|F_i^{-1} g_i\|_2^2. \quad (10)$$
  
296

297  
298 **Theorem 3.** *Let  $C^* \in \arg \max_{C \subseteq N} A_C(s, a_C)$ . Under the strong  $\epsilon$ -Core,  $\sum_{i \notin C^*} A_i \leq \epsilon$  and thus  
299  $\Delta \log \pi_{N \setminus C^*}(a_{N \setminus C^*} | s) \lesssim \alpha \epsilon$ , while  $\Delta \log \pi_{C^*}(a_{C^*} | s) \gtrsim \alpha (A_{C^*} - \epsilon)$ .*300  
301 Solving the quadratic programming problem (8) requires  $2^{|N|}$  inferences of the value network to  
302 obtain  $\mathbb{E}_{a_{N \setminus C}}[Q(s, a_C, a_{N \setminus C})]$  or  $Q(s, a_C, \bar{a}_{N \setminus C})$  for each coalition  $C \subseteq N$ . This may result  
303 in significant computational overhead for large-scale problems. To address this issue, our method  
304 randomly samples a relatively small number of coalitions  $\mathcal{C} = \{C_1, C_2, \dots, C_m\}$  and computes the  
305 desired solution satisfying the constraints of these coalitions, resulting in the quadratic programming  
306 19. Theorem 4 shows that its approximation error can be controlled by the sample size  $m$ .307  
308 **Theorem 4.** *Given a distribution  $\mathcal{P}$  over  $2^N$ , and  $\delta, \Delta > 0$ , solving the programming (19) over  
309  $O((n + 2 + \log(1/\Delta))/\delta^2)$  coalitions sampled from  $\mathcal{P}$  gives an allocation vector in the  $\delta$ -probable  
core with probability  $1 - \Delta$ .*310  
311 The above proof is for the general form of  $A_C(s, a_C)$ . For a more rigorous approach, we use the  
312 detailed definition  $A_C(s, a_C) = \mathbb{E}_{a_{N \setminus C} \sim \pi_{N \setminus C}}[Q(s, a_C, a_{N \setminus C})] - V(s)$ . Using the PPO/TRPO  
313 framework, we arrive at the following conclusions.314  
315 **Theorem 5.** *Given a factored joint policy  $\pi(a | s) = \prod_{i \in N} \pi_i(a_i | s)$  and the CORA advantage  
316 allocation satisfying the coalition constraint*

317  
318 
$$\sum_{j \in C} A_j(s, a) \geq A_C(s, a_C) - \epsilon, \quad \forall C \subseteq N,$$

319  
320 *the following hold for the trust-region penalized policy update with parameter  $\eta > 0$ .*321  
322 **(1) Individual improvement lower bound.** *Assume  $m_i \leq A_i(s, a) \leq M_i$  with  $R_i = M_i - m_i$ .  
323 Then each agent satisfies*

324  
325 
$$\Delta \log \pi_i(a_i | s) \geq \eta(A_i(s, a) - \epsilon) - \frac{\eta^2 R_i^2}{8}.$$

324 **(2) Coalition improvement lower bound.** For any coalition  $C \subseteq N$ ,

$$326 \quad \Delta \log \pi_C(a_C | s) \geq \eta(A_C(s, a_C) - (1 + |C|)\epsilon) - \sum_{i \in C} \frac{\eta^2 R_i^2}{8}.$$

329 These bounds imply that CORA protects high-value coalitions by enforcing a guaranteed positive  
330 advantage contribution even when the global joint advantage  $A_N(s, a)$  is weak or negative.

## 333 6 EXPERIMENTS

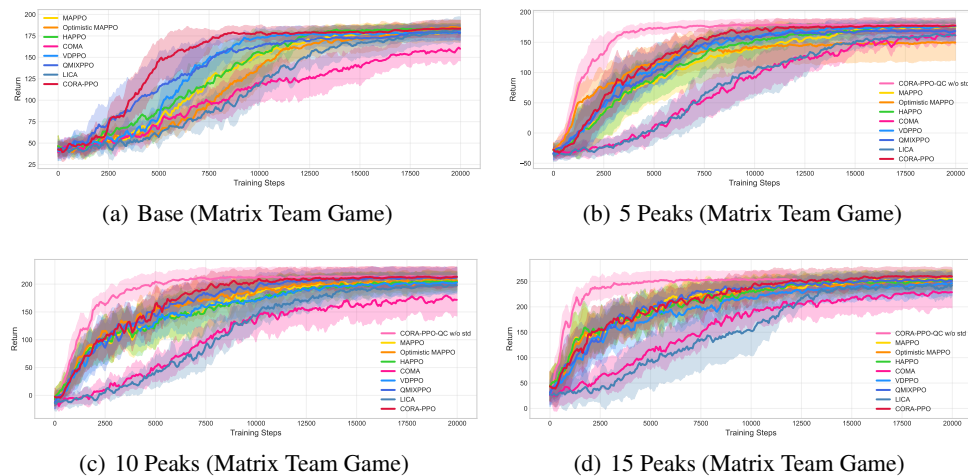
335 We evaluate the CORA method across several multi-agent environments, including matrix games,  
336 differential games, the VMAS simulator Bettini et al. (2022), the Multi-Agent MuJoCo (MaMujoco)  
337 environment de Lazcano et al. (2024); Kuba et al. (2021), and the Starcraft Multi-Agent Challenge  
338 (SMAC) environment Samvelyan et al. (2019); Hu et al. (2023).

### 340 6.1 MATRIX GAMES

342 In this section, we construct two types of matrix-style cooperative game environments to evaluate  
343 the fundamental performance of different algorithms.

344 **Matrix Team Game (MTG):** In this environment, agents receive a shared reward at each time step  
345 based on their joint action, determined by a randomly generated reward matrix. Each element of  
346 the matrix is uniformly sampled from the interval  $[-10, 20]$ . The game proceeds for 10 steps per  
347 episode. Each agent observes a global one-hot encoded state indicating the current step number,  
348 allowing them to learn time-dependent coordination strategies.

349 **Multi-Peak Matrix Team Game:** To further evaluate each algorithm’s ability to optimize coop-  
350 erative strategies in environments with multiple local optima, we extend MTG to design a more  
351 challenging setting. The matrix is filled with background noise in the range  $[-10, 0]$ , overlaid with  
352 multiple reward peaks. Among them, one peak is the global optimum (highest value), while the rest  
353 are local optima. Actions deviating from peak combinations incur heavy penalties due to the nega-  
354 tive background. This setting is designed to test whether algorithms can escape suboptimal solutions  
355 and discover globally coordinated strategies.



373 Figure 1: Training performance on Matrix Team Game and its Multi-Peak variants with 5, 10, and  
374 15 reward peaks.

376 As shown in Figure 1, CORA exhibits faster convergence and higher returns compared to the base-  
377 line algorithms, demonstrating superior coordination and learning efficiency in this simple and gen-  
378 eral environment. As a comparison, we also implemented a quadratic critic that directly parameter-

378 izes the joint action value as a quadratic form:

379

$$380 Q(s, a) = b(s) + \sum_i \langle u_i(s), a_i \rangle + \sum_{i < j} a_i^\top W_{ij}(s) a_j,$$

381

382 where  $a_i$  is the one-hot or probabilistic action vector of agent  $i$ . This representation allows us to  
383 evaluate coalition values in closed form with baseline  $a_i \sim \pi_i(a_i|s)$  for  $i \notin C$ , e.g.,

384

$$385 Q_C(s, a_C) = \mathbb{E}_{a_{N \setminus C} \sim \pi_{N \setminus C}} [Q(s, a_C, a_{N \setminus C})],$$

386

387 by simply replacing the action inputs of non-coalition agents with their policy distributions. The  
388 results, shown as CORA-PPO-QC, confirm this gap and highlight the stability advantage of CORA.

389

## 390 6.2 DIFFERENTIAL GAMES

391

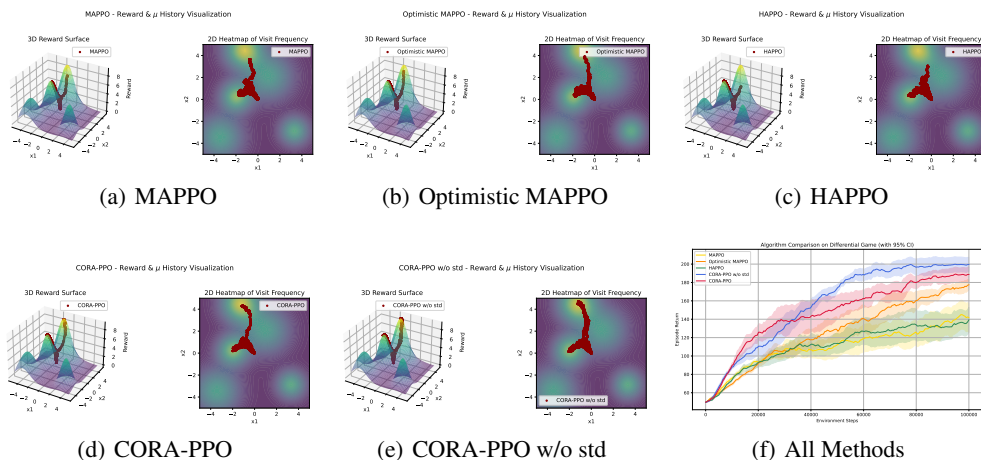
392 To demonstrate the learning process, we designed a 2D differential game environment (similar to  
(Wei & Luke, 2016)). Each agent selects an action  $x_1, x_2 \in [-5, 5]$  at every step. The reward  
393 function  $R(x_1, x_2)$  is composed of a sum of several two-dimensional Gaussian potential fields,  
394 defined as:

395

$$396 R(x_1, x_2) = \sum_{i=1}^n h_i \cdot \exp \left( -\frac{(x_1 - c_{x_i})^2 + (x_2 - c_{y_i})^2}{\sigma_i^2} \right) \quad (11)$$

397 Here,  $n$  is the number of fields,  $(c_{x_i}, c_{y_i})$  is the center of the  $i$ -th potential field,  $h_i \in [5, 10]$  indicates  
398 the peak height of the potential field, and  $\sigma_i \in [1, 2]$  controls its spread. This setup results in  
399 an environment with multiple local optima, presenting significant strategy exploration and learning  
400 challenges for MARL algorithms. The environment state itself does not evolve and can be regarded  
401 as a repeated single-step game. Key parameters like location, height, width of potential fields are set  
402 by a random seed.

403



418 Figure 2: The reward and learning trajectories of various algorithms in the differential game scenario  
419 ( $\mu$  in Gaussian strategy).

420

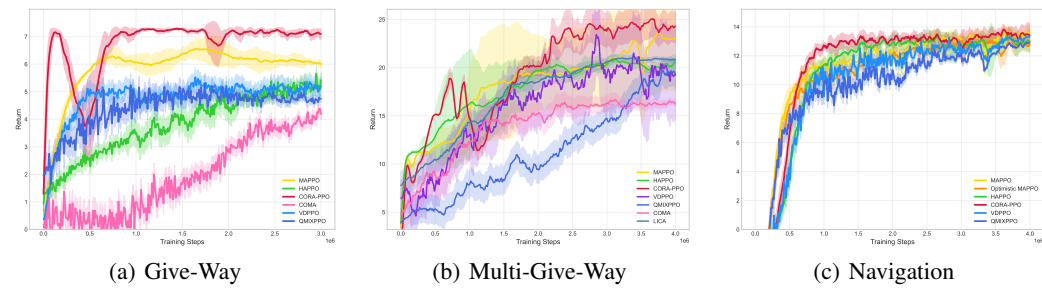
421 Figure 2(f) shows the performance of MAPPO, HAPPO, CORA-PPO, CORA-PPO without std, and  
422 Optimistic MAPPO in this environment. CORA-PPO demonstrates the best learning speed and  
423 performance, and CORA-PPO without std outperforms other algorithms. We believe this is because  
424 the std term somewhat suppresses agent exploration. Since the differential game has multiple local  
425 optima, the std term constrains exploration across these optima. Furthermore, thanks to the theory  
426 of Optimistic Q-learning, Optimistic MAPPO also outperforms both HAPPO and MAPPO in this  
427 environment.

428

429 The detailed learning trajectories are visualized in Figure 2, which illustrate the learning trajectories  
430 of various methods during training (through the mean  $\mu_i$  in the Gaussian policy  $N(\mu_i, \sigma_i)$ ). It is  
431 clearly visible that the CORA-PPO series effectively promotes agents to learn optimal cooperative  
432 strategies (reaching the peak in the 3D Reward Surface; reaching the brightest point in the 2D  
433 Heatmap).

432 6.3 VMAS  
433

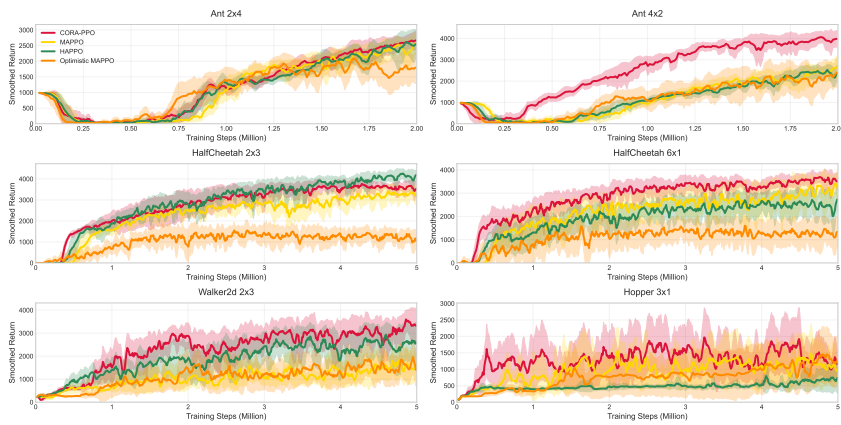
434 VMAS (Vectorized Multi-Agent Simulator) is a PyTorch-based vectorized multi-agent simulator  
435 designed for efficient multi-agent reinforcement learning benchmarking Bettini et al. (2022; 2024);  
436 Bou et al. (2023). It provides a range of challenging multi-agent scenarios, and utilizes GPU acceleration,  
437 making it suitable for large-scale MARL training. We selected the following scenarios for  
438 testing: **Multi-Give-Way**: Four agents must coordinate to cross a shared corridor by giving way to  
439 each other to reach their respective goals. **Give-Way**: Two agents are placed in a narrow corridor  
440 with goals on opposite ends. Success requires one agent to yield and allow the other to pass first,  
441 reflecting asymmetric cooperative behavior. **Navigation**: Agents are randomly initialized and must  
442 navigate to their own goals while avoiding collisions. These tasks require strong coordination and  
443 implicit role assignment.

444  
445 Figure 3: Training performance on the VMAS scenarios.  
446

447 As shown in Figure 3, CORA achieves higher returns and more stable performance compared to the  
448 other algorithms.

449 6.4 MULTI-AGENT MUJOCO  
450

451 To demonstrate the effectiveness of CORA in continuous control tasks, we conducted experiments  
452 on the popular benchmark Multi-Agent MuJoCo (MA-MuJoCo) Kuba et al. (2021), using its latest  
453 version, MaMuJoCo-v5 de Lazcano et al. (2024).

454  
455 Figure 4: Training performance in the Multi-Agent MuJoCo (MaMuJoCo-v5) scenario.  
456

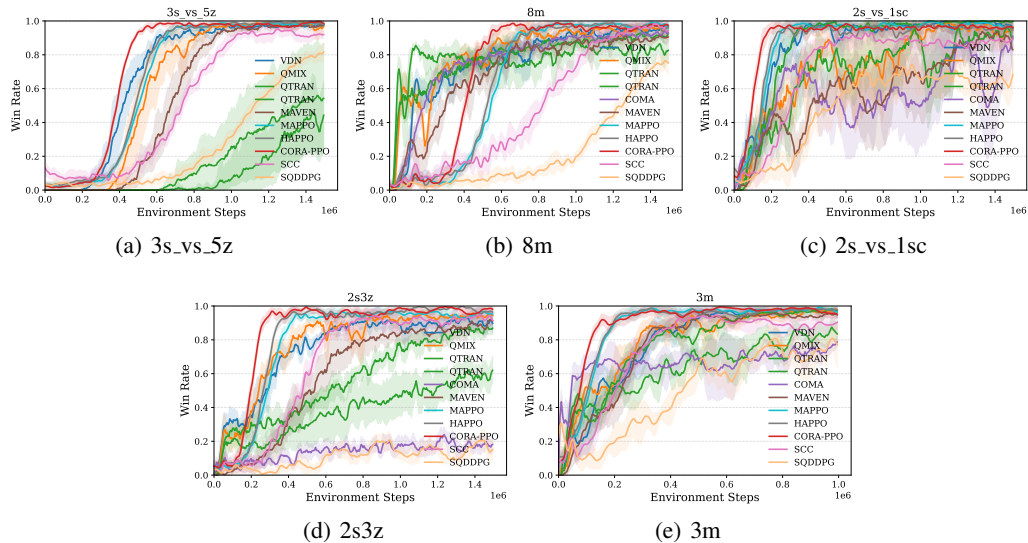
457 As shown in Figure 4, CORA-PPO achieves state-of-the-art performance across multiple scenarios.  
458 Except for the *HalfCheetah 2x3* task where HAPPO slightly outperforms, CORA-PPO demonstrates  
459 superior results in the *Ant 4x2*, *HalfCheetah 6x1*, *Walker2d 2x3*, and *Hopper 3x1* tasks. These results  
460 highlight the effectiveness of CORA in handling diverse and challenging multi-agent continuous  
461 control environments.

## 486 6.5 STARCRAFT MULTI-AGENT CHALLENGE (SMAC)

488 We further validate the scalability and cooperation capability of CORA-PPO on the StarCraft Multi-  
 489 Agent Challenge (SMAC). All experiments are conducted using SC2 version 4.10 under decentral-  
 490 ized execution with global team reward, following standard protocols. Results are averaged over 8  
 491 runs with 95% confidence intervals.

492 Five representative maps of different cooperative difficulty are selected: 3s\_vs\_5z, 8m, 2s\_vs\_1sc,  
 493 2s3z, and 3m. These maps involve heterogeneous team sizes, spatial complexity, and micro-control  
 494 demands, creating challenges in credit assignment and coordinated tactics.

495 Figures 5(a)–5(e) show that CORA-PPO consistently achieves higher win rates and faster conver-  
 496 gence than MAPPO and HAPPO. In the more demanding maps (3s\_vs\_5z and 2s\_vs\_1sc), CORA-  
 497 PPO notably enhances cooperative unit control and improves asymptotic performance, demon-  
 498 strating its robustness in partial observability and high-interaction combat.

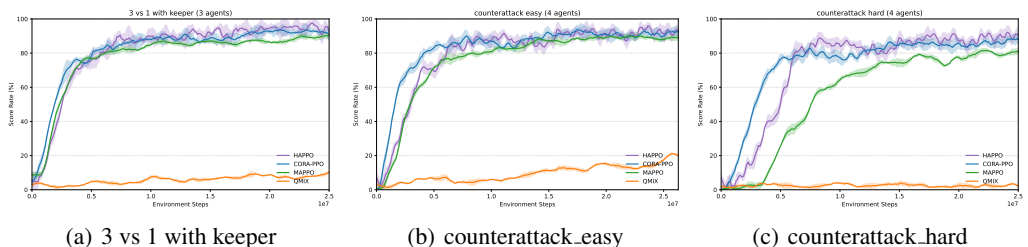


518 Figure 5: Win rate comparison across SMAC scenarios.

## 521 6.6 GOOGLE RESEARCH FOOTBALL

523 We further evaluate CORA-PPO on the Google Research Football (GRF) benchmark. Results are  
 524 averaged over 8 random seeds with 95% confidence intervals.

525 We consider three representative cooperative tasks: *3 vs 1 with keeper* (3 agents), *counter-  
 526 attack\_easy*, and *counterattack\_hard*. As shown in Figures 6(a)–6(c), CORA-PPO achieves higher  
 527 returns and more stable training, indicating that coalition-aware credit assignment improves cooper-  
 528 ative decision-making under sparse and delayed rewards.



539 Figure 6: Performance comparison on GRF scenarios.

540 ETHICS STATEMENT  
541542 We have read and will adhere to the ICLR Code of Ethics. This work does not involve human  
543 subjects, personally identifiable information, or sensitive attributes. No new datasets with personal  
544 data are collected. Experiments are conducted in standard public benchmarks under their respective  
545 licenses.546 Potential negative societal impacts: our method could be used to optimize multi-agent coordina-  
547 tion in safety-critical or competitive scenarios. To mitigate risks, we (i) avoid claims beyond mea-  
548 sured settings; (ii) release only research artifacts necessary to reproduce results; and (iii) encourage  
549 deployment-time safeguards (e.g., monitoring, intervention policies). We are unaware of legal com-  
550 pliance issues specific to the presented experiments.551 Conflicts of interest: none declared.  
552553  
554 REPRODUCIBILITY STATEMENT  
555556 We take the following steps to support reproducibility. (1) **Algorithm details.** CORA's objective  
557 and constraints are specified in Sec. 4.2 (Eq. 8, 19); the policy-gradient estimator and baselines  
558 are defined in Sec. 3. (2) **Implementation.** Pseudocode is provided in 1. (3) **Hyperparam-**  
559 **eters.** Complete training hyperparameters per environment are listed in Table 1 (actor/critic learning  
560 rates,  $\gamma$ , GAE  $\lambda$ , PPO clip, parallel envs, epochs). (4) **Environments & seeds.** We describe ma-  
561 trix/differential games, VMAS, and Multi-Agent MuJoCo settings in Sec. 6 and Appendix, including  
562 action/state spaces, reward definitions, and episode lengths. We run 5 random seeds for both envi-  
563 ronment and algorithm initializations and report mean with 95% confidence intervals. (5) **Code &**  
564 **artifacts.** Anonymized code and configuration files (including environment wrappers and plotting  
565 scripts) will be provided in the supplementary materials; instructions include exact package versions,  
566 and commands to reproduce all figures. (6) **Ablations.** We report the effect of coalition sample size  
567 and the variance regularizer in Appendix (Fig. 8, 9).568 REFERENCES  
569

- 570 Matteo Bettini, Ryan Kortvelesy, Jan Blumenkamp, and Amanda Prorok. Vmas: A vectorized multi-
- 
- 571 agent simulator for collective robot learning.
- The 16th International Symposium on Distributed*
- 
- 572
- Autonomous Robotic Systems*
- , 2022.
- 
- 573
- 
- 574 Matteo Bettini, Ryan Kortvelesy, and Amanda Prorok. Controlling behavioral diversity in multi-
- 
- 575 agent reinforcement learning. In
- Forty-first International Conference on Machine Learning*
- , 2024.
- 
- 576 URL
- <https://openreview.net/forum?id=qQjUgItPq4>
- .
- 
- 577
- 
- 578 Albert Bou, Matteo Bettini, Sebastian Dittert, Vikash Kumar, Shagun Sodhani, Xiaomeng Yang,
- 
- 579 Gianni De Fabritiis, and Vincent Moens. Torchrl: A data-driven decision-making library for
- 
- 580 pytorch, 2023.
- 
- 581
- 
- 582 Lucian Busoniu, Robert Babuska, and Bart De Schutter. A comprehensive survey of multiagent rein-
- 
- 583 forcement learning.
- IEEE Transactions on Systems, Man, and Cybernetics, Part C (Applications*
- 
- 584
- and Reviews)*
- , 38(2):156–172, 2008.
- 
- 585
- 
- 586 Bhaskar Ray Chaudhury, Linyi Li, Mintong Kang, Bo Li, and Ruta Mehta. Fairness in federated
- 
- 587 learning via core-stability. In
- Proceedings of Advances in Neural Information Processing Systems*
- ,
- 
- 588 pp. 5738–5750, 2022.
- 
- 589
- 
- 590 Sirui Chen, Zhaowei Zhang, Yaodong Yang, and Yali Du. Stas: Spatial-temporal return decom-
- 
- 591 position for multi-agent reinforcement learning. In
- The Annual AAAI Conference on Artificial*
- 
- 592
- Intelligence*
- , 2024.
- 
- 593
- 
- 594 Rodrigo de Lazcano, Kallinteris Andreas, Jun Jet Tai, Seungjae Ryan Lee, and Jordan
- 
- 595 Terry. Gymnasium robotics, 2024. URL
- <http://github.com/Farama-Foundation/Gymnasium-Robotics>
- .

- 594 Kate Donahue and Jon M. Kleinberg. Optimality and stability in federated learning: A game-  
 595 theoretic approach. In *Proceedings of Advances in Neural Information Processing Systems*, pp.  
 596 1287–1298, 2021.
- 597
- 598 Theo SH Driessens. *Cooperative games, solutions and applications*. Springer Science and Business  
 599 Media, 2013.
- 600 Jakob Foerster, Gregory Farquhar, Triantafyllos Afouras, Nantas Nardelli, and Shimon Whiteson.  
 601 Counterfactual multi-agent policy gradients. In *Proceedings of the AAAI conference on artificial  
 602 intelligence*, volume 32, 2018.
- 603
- 604 Amirata Ghorbani and James Zou. Data shapley: Equitable valuation of data for machine learning.  
 605 In *Proceedings of International Conference on Machine Learning*, pp. 2242–2251, 2019.
- 606 Siyi Hu, Yifan Zhong, Minquan Gao, Weixun Wang, Hao Dong, Xiaodan Liang, Zhihui Li, Xiaojun  
 607 Chang, and Yaodong Yang. Marllib: A scalable and efficient multi-agent reinforcement learning  
 608 library. *Journal of Machine Learning Research*, 2023.
- 609
- 610 Ruoxi Jia, David Dao, Boxin Wang, Frances Ann Hubis, Nick Hynes, Nezihe Merve Gürel, Bo Li,  
 611 Ce Zhang, Dawn Song, and Costas J Spanos. Towards efficient data valuation based on the shapley  
 612 value. In *Proceedings of International Conference on Artificial Intelligence and Statistics*, pp.  
 613 1167–1176, 2019.
- 614 Jakub Grudzien Kuba, Ruiqing Chen, Muning Wen, Ying Wen, Fanglei Sun, Jun Wang, and Yaodong  
 615 Yang. Trust region policy optimisation in multi-agent reinforcement learning. *arXiv preprint  
 616 arXiv:2109.11251*, 2021.
- 617
- 618 Jiahui Li, Kun Kuang, Baoxiang Wang, Furui Liu, Long Chen, Fei Wu, and Jun Xiao. Shapley  
 619 counterfactual credits for multi-agent reinforcement learning. In *Proceedings of the 27th ACM  
 620 SIGKDD Conference on Knowledge Discovery & Data Mining*, pp. 934–942, 2021.
- 621 Michael L. Littman. Markov games as a framework for multi-agent reinforcement learning. In  
 622 William W. Cohen and Haym Hirsh (eds.), *Machine Learning Proceedings 1994*, pp. 157–163.  
 623 Morgan Kaufmann, 1994. doi: 10.1016/B978-1-55860-335-6.50027-1.
- 624 Ryan Lowe, Yi I Wu, Aviv Tamar, Jean Harb, OpenAI Pieter Abbeel, and Igor Mordatch. Multi-  
 625 agent actor-critic for mixed cooperative-competitive environments. *Advances in neural informa-  
 626 tion processing systems*, 30, 2017.
- 627
- 628 Chengdong Ma, Aming Li, Yali Du, Hao Dong, and Yaodong Yang. Efficient and scalable reinforce-  
 629 ment learning for large - scale network control. *Nature Machine Intelligence*, 6(9):1006–1020, 09  
 630 2024. ISSN 2522-5839. doi: 10.1038/s42256-024-00879-7.
- 631
- 632 Frans A. Oliehoek, Matthijs T. J. Spaan, and Nikos Vlassis. Optimal and approximate q-value  
 633 functions for decentralized pomdps. *J. Artif. Int. Res.*, 32(1):289–353, May 2008.
- 634
- 635 Liviu Panait and Sean Luke. Cooperative multi-agent learning: The state of the art. *Auton Agent  
 636 Multi-Agent Syst*, 11:387–434, 2005. doi: 10.1007/s10458-005-2631-2.
- 637
- 638 Bei Peng, Tabish Rashid, Christian Schroeder de Witt, Pierre-Alexandre Kamienny, Philip Torr,  
 639 Wendelin Böhmer, and Shimon Whiteson. Facmac: Factored multi-agent centralised policy gra-  
 640 dients. *Advances in Neural Information Processing Systems*, 34:12208–12221, 2021.
- 641
- 642 Tabish Rashid, Mikayel Samvelyan, Christian Schroeder, Gregory Farquhar, Jakob Foerster, and  
 643 Shimon Whiteson. Qmix: Monotonic value function factorisation for deep multi-agent reinforce-  
 644 ment learning. In *International conference on machine learning*, pp. 4295–4304. PMLR, 2018.
- 645
- 646 Mikayel Samvelyan, Tabish Rashid, Christian Schroeder De Witt, Gregory Farquhar, Nantas  
 647 Nardelli, Tim GJ Rudner, Chia-Man Hung, Philip HS Torr, Jakob Foerster, and Shimon Whiteson.  
 648 The starcraft multi-agent challenge. *arXiv preprint arXiv:1902.04043*, 2019.
- 649
- 650 John Schulman, Filip Wolski, Prafulla Dhariwal, Alec Radford, and Oleg Klimov. Proximal policy  
 651 optimization algorithms. *arXiv preprint arXiv:1707.06347*, 2017.

- 648 Shai Shalev-Shwartz, Shaked Shammah, and Shai Amnon. Safe, multi-agent, reinforcement learning  
 649 for autonomous driving, 2016.
- 650
- 651 Jennifer She, Jayesh K. Gupta, and Mykel J.i Kochenderfer. Agent-time attention for sparse re-  
 652 wards multi-agent reinforcement learning. In *International Conference on Autonomous Agents  
 653 and Multiagent Systems*, 2022.
- 654 Rachael Hwee Ling Sim, Yehong Zhang, Mun Choon Chan, and Bryan Kian Hsiang Low. Collab-  
 655 orative machine learning with incentive-aware model rewards. In *Proceedings of International  
 656 Conference on Machine Learning*, pp. 8927–8936, 2020.
- 657
- 658 Kyunghwan Son, Daewoo Kim, Wan Ju Kang, David Earl Hostallero, and Yung Yi. Qtran: Learning  
 659 to factorize with transformation for cooperative multi-agent reinforcement learning. In *Interna-  
 660 tional conference on machine learning*, pp. 5887–5896. PMLR, 2019.
- 661 Jianyu Su, Stephen Adams, and Peter Beling. Value-decomposition multi-agent actor-critics. In  
 662 *Proceedings of the AAAI conference on artificial intelligence*, volume 35, pp. 11352–11360, 2021.
- 663
- 664 Peter Sunehag, Guy Lever, Audrunas Gruslys, Wojciech Marian Czarnecki, Vinicius Zambaldi, Max  
 665 Jaderberg, Marc Lanctot, Nicolas Sonnerat, Joel Z Leibo, Karl Tuyls, et al. Value-decomposition  
 666 networks for cooperative multi-agent learning. *arXiv preprint arXiv:1706.05296*, 2017.
- 667 J. Wang, Y. Zhang, T.-K. Kim, and Y. Gu. Shapley q-value: A local reward approach to solve global  
 668 reward games. *Proceedings of the AAAI Conference on Artificial Intelligence*, 34(05):7285–7292,  
 669 2020a. doi: 10.1609/aaai.v34i05.6220.
- 670
- 671 Jianhao Wang, Zhizhou Ren, Terry Liu, Yang Yu, and Chongjie Zhang. Qplex: Duplex dueling  
 672 multi-agent q-learning. *arXiv preprint arXiv:2008.01062*, 2020b.
- 673
- 674 Jianhong Wang, Yuan Zhang, Yunjie Gu, and Tae-Kyun Kim. Shaq: Incorporating shapley value  
 675 theory into multi-agent q-learning. *Advances in Neural Information Processing Systems*, 35:  
 5941–5954, 2022a.
- 676
- 677 Li Wang, Yupeng Zhang, Yujing Hu, Weixun Wang, Chongjie Zhang, Yang Gao, Jianye Hao, Tangjie  
 678 Lv, and Changjie Fan. Individual reward assisted multi-agent reinforcement learning. In Kamalika  
 679 Chaudhuri, Stefanie Jegelka, Le Song, Csaba Szepesvári, Gang Niu, and Sivan Sabato (eds.),  
 680 *International Conference on Machine Learning, ICML 2022, 17-23 July 2022, Baltimore, Mary-  
 681 land, USA*, volume 162 of *Proceedings of Machine Learning Research*, pp. 23417–23432. PMLR,  
 682 2022b. URL <https://proceedings.mlr.press/v162/wang22ao.html>.
- 683
- 684 Tonghan Wang, Tarun Gupta, Anuj Mahajan, Bei Peng, Shimon Whiteson, and Chongjie Zhang.  
 Rode: Learning roles to decompose multi-agent tasks. *arXiv preprint arXiv:2010.01523*, 2020c.
- 685
- 686 Yihan Wang, Beining Han, Tonghan Wang, Heng Dong, and Chongjie Zhang. Dop: Off-policy  
 687 multi-agent decomposed policy gradients. In *International conference on learning representa-  
 688 tions*, 2020d.
- 689
- 690 Ermo Wei and Sean Luke. Lenient learning in independent-learner stochastic cooperative games.  
 691 *Journal of Machine Learning Research*, 17(84):1–42, 2016. URL <http://jmlr.org/papers/v17/15-417.html>.
- 692
- 693 Tom Yan and Ariel D Procaccia. If you like shapley then you'll love the core. In *Proceedings of the  
 694 AAAI Conference on Artificial Intelligence*, pp. 5751–5759, 2021.
- 695
- 696 Chao Yu, Akash Velu, Eugene Vinitsky, Jiaxuan Gao, Yu Wang, Alexandre Bayen, and Yi Wu.  
 697 The surprising effectiveness of ppo in cooperative multi-agent games. In *Advances in Neural  
 698 Information Processing Systems*, volume 35, pp. 24611–24624. Curran Associates, Inc., 2022.
- 699
- 700 Wenshuai Zhao, Yi Zhao, Zhiyuan Li, Juho Kannala, and Joni Pajarinen. Optimistic multi-agent  
 701 policy gradient. In *Proceedings of the International Conference on Machine Learning*, 2024.
- 702
- 703 Yifan Zhong, Jakub Grudzien Kuba, Siyi Hu, Jiaming Ji, and Yaodong Yang. Heterogeneous-agent  
 704 reinforcement learning, 2023.

702 Meng Zhou, Ziyu Liu, Pengwei Sui, Yixuan Li, and Yuk Ying Chung. Learning implicit credit  
 703 assignment for cooperative multi-agent reinforcement learning. *arXiv preprint arXiv:2007.02529*,  
 704 2020.

## 707 A APPENDIX

709 In this appendix, we provide detailed statements of the theorems, lemmas, and their corresponding  
 710 proofs presented in the main text.

### 712 A.1 PRELIMINARIES AND NOTATION

714 The actor parameters are  $\phi = (\phi_1, \dots, \phi_n)$  and the factored joint policy  $\pi_\phi(a | s) = \prod_{i=1}^n \pi_i(a_i |$   
 715  $s; \phi_i)$ . Define score features and per-agent Fisher matrices

$$716 \psi_i(s, a_i) := \nabla_{\phi_i} \log \pi_i(a_i | s), \quad F_i := \mathbb{E}[\psi_i \psi_i^\top], \quad F = \text{diag}(F_1, \dots, F_n) \succeq 0.$$

718 The NPG step is

$$719 \phi'_i = \phi_i + \alpha F_i^{-1} g_i, \quad g_i := \mathbb{E}[\psi_i A_i], \quad (12)$$

720 for step size  $\alpha > 0$ . Global advantage  $A_N(s, a) := Q(s, a) - V(s)$  and coalitional advantage  
 721  $A_C(s, a_C)$ . A credit allocation  $\{A_i\}_{i \in N}$  satisfies the strong  $\epsilon$ -Core if

$$722 \sum_{i \in N} A_i = A_N, \quad \sum_{i \in C} A_i \geq A_C(s, a_C) - \epsilon, \quad \forall C \subseteq N. \quad (13)$$

### 725 A.2 COMPATIBLE FUNCTION APPROXIMATION

727 **Definition 6** (Compatible approximation). For agent  $i$ , consider  $\mathcal{S}_i = \{w_i^\top \psi_i : w_i \in \mathbb{R}^{d_i}\}$ . We say  
 728  $A_i$  is compatibly representable if

$$730 w_i^* = \arg \min_w \mathbb{E}[(A_i - w^\top \psi_i)^2]$$

732 exists and satisfies the normal equation  $\mathbb{E}[\psi_i A_i] = \mathbb{E}[\psi_i \psi_i^\top] w_i^* = F_i w_i^*$ .

733 **Lemma 7.** With  $g_i = \mathbb{E}[\psi_i A_i]$ , the NPG step equation 12 gives  $\phi'_i - \phi_i = \alpha F_i^{-1} g_i = \alpha w_i^*$ .

735 *Proof.* From  $F_i w_i^* = g_i$ , left-multiply by  $F_i^{-1}$  to obtain  $w_i^* = F_i^{-1} g_i$ . Substitute into equation 12.  $\square$

737 **Lemma 8.** For small  $\alpha$ , the Taylor expansion yields

$$739 \Delta \log \pi_i(a_i | s) := \log \pi'_i(a_i | s) - \log \pi_i(a_i | s) \approx \psi_i(s, a_i)^\top (\phi'_i - \phi_i).$$

741 *Proof.* Differentiate  $\log \pi_i(a_i | s; \phi_i)$  at  $\phi_i$  in direction  $(\phi'_i - \phi_i)$ .  $\square$

### 743 A.3 FIRST-ORDER CHANGES

745 **Theorem 1'.** Under compatible approximation and equation 12,

$$747 \Delta \log \pi_i(a_i | s) \approx \alpha A_i, \quad (14)$$

$$748 \Delta \log \pi(a | s) = \sum_{i=1}^n \Delta \log \pi_i(a_i | s) \approx \alpha A_N, \quad (15)$$

$$751 \Delta \log \pi_C(a_C | s) = \sum_{i \in C} \Delta \log \pi_i(a_i | s) \approx \alpha \sum_{i \in C} A_i. \quad (16)$$

754 *Proof.* By Lemma 8 and Lemma 7,  $\Delta \log \pi_i \approx \psi_i^\top (\alpha w_i^*) = \alpha w_i^{*\top} \psi_i = \alpha A_i$ , which proves  
 755 equation 14. Because  $\log \pi = \sum_i \log \pi_i$ , summing equation 14 over  $i$  and using  $\sum_i A_i = A_{tot}(s, a)$   
 yields equation 15. Similarly,  $\log \pi_C = \sum_{i \in C} \log \pi_i$  gives equation 16.  $\square$

756 **Corollary 9.** Using  $\Delta\pi(\cdot) \approx \pi(\cdot)\Delta\log\pi(\cdot)$ ,  $\Delta\pi(a \mid s) \approx \alpha\pi(a \mid s)A_N$  and  $\Delta\pi_C(a_C \mid s) \approx$   
 757  $\alpha\pi_C(a_C \mid s)\sum_{i \in C} A_i$ .

759 *Remark 1* (If  $A_i \notin \mathcal{S}_i$ ). All first-order relations remain valid with  $A_i$  replaced by its  $L^2$  projection  
 760 onto  $\mathcal{S}_i$ . Operationally, NPG realizes this via  $w_i^* = F_i^{-1}\mathbb{E}[\psi_i A_i]$ .

#### 761 A.4 COALITIONAL LOWER BOUNDS FROM THE STRONG $\epsilon$ -CORE

764 **Theorem 2'.** Consider one NPG step  $\phi'_i = \phi_i + \alpha F_i^{-1}g_i$  with  $g_i := \mathbb{E}[\psi_i A_i]$ ,  $\psi_i := \nabla_{\phi_i} \log \pi_i(a_i \mid$   
 765  $s)$ ,  $F_i := \mathbb{E}[\psi_i \psi_i^\top]$ , and step size  $\alpha > 0$ . Assume for each agent  $i$  that  $\log \pi_i(\cdot \mid s; \phi_i)$  is twice  
 766 continuously differentiable and its Hessian is uniformly bounded on the line segment between  $\phi_i$  and  $\phi'_i$ :

$$768 \|\nabla_{\phi_i}^2 \log \pi_i(a_i \mid s; \xi_i)\|_{\text{op}} \leq L_i \quad \text{for all } \xi_i \in [\phi_i, \phi'_i].$$

770 Then for any coalition  $C \subseteq N$  and any sampled  $(s, a)$ ,

$$771 \Delta \log \pi_C(a_C \mid s) \geq \alpha \sum_{i \in C} A_i - \frac{\alpha^2}{2} \sum_{i \in C} L_i \|F_i^{-1}g_i\|_2^2. \quad (17)$$

774 If, in addition, the strong  $\epsilon$ -Core constraints hold,  $\sum_{i \in C} A_i \geq A_C(s, a_C) - \epsilon$ , then

$$777 \Delta \log \pi_C(a_C \mid s) \geq \alpha(A_C(s, a_C) - \epsilon) - \frac{\alpha^2}{2} \sum_{i \in C} L_i \|F_i^{-1}g_i\|_2^2. \quad (18)$$

780 *Proof.* For each  $i$ , apply the second-order Taylor expansion of  $\log \pi_i(a_i \mid s; \phi_i)$  along the direction  
 781  $\Delta\phi_i := \phi'_i - \phi_i$ :

$$783 \Delta \log \pi_i(a_i \mid s) = \psi_i(s, a_i)^\top \Delta\phi_i + \frac{1}{2} \Delta\phi_i^\top (\nabla_{\phi_i}^2 \log \pi_i(a_i \mid s; \xi_i)) \Delta\phi_i,$$

785 for some  $\xi_i$  on the line segment between  $\phi_i$  and  $\phi'_i$ . With  $\Delta\phi_i = \alpha F_i^{-1}g_i$  and the operator-norm  
 786 bound on the Hessian,

$$788 \Delta \log \pi_i(a_i \mid s) \geq \alpha \psi_i^\top F_i^{-1}g_i - \frac{\alpha^2}{2} L_i \|F_i^{-1}g_i\|_2^2.$$

791 By compatible approximation,  $\psi_i^\top F_i^{-1}g_i = A_i$ . Summing over  $i \in C$  yields equation 17. Combin-  
 792 ing with the strong  $\epsilon$ -Core inequality gives equation 18.  $\square$

#### 794 A.5 ADVANTAGE CONCENTRATION ON A MAXIMIZING COALITION

796 Let  $C^* \in \arg \max_{C \subseteq N} A_C(s, a_C)$ , we have  $A_{C^*} \geq A_N$ .

797 **Theorem 3'.** Under equation 13:

$$799 1. \sum_{i \notin C^*} A_i = A_N - \sum_{i \in C^*} A_i \leq A_N - (A_{C^*} - \epsilon) \leq \epsilon, \text{ hence } \Delta \log \pi_{N \setminus C^*}(a_{N \setminus C^*} \mid s) \lesssim \alpha \epsilon.$$

$$802 2. \Delta \log \pi_{C^*}(a_{C^*} \mid s) \gtrsim \alpha(A_{C^*} - \epsilon).$$

804 *Proof.* (1) From  $\sum_{i \in C^*} A_i \geq A_{C^*} - \epsilon$  and  $A_{C^*} \geq A_N$ ,  $\sum_{i \notin C^*} A_i \leq \epsilon$ ; then apply equation 16 to  
 805 the complement. (2) This is equation 15.  $\square$

#### 808 A.6 THEOREM 4: APPROXIMATION WITH SAMPLED COALITIONS

809 The approximate quadratic programming problem mentioned in the main text is as follows.

$$\begin{aligned}
& \underset{\epsilon \geq 0, A_1, \dots, A_n}{\text{minimize}} \quad \epsilon + \lambda \sum_{i \in N} \left( A_i - \frac{1}{|N|} A_N \right)^2, \\
& \text{subject to: } \sum_{i \in N} A_i = A_N, \\
& \quad \sum_{i \in C_k} A_i \geq A_{C_k}(s, a_{C_k}) - \epsilon, \forall C_k \in \mathcal{C}.
\end{aligned} \tag{19}$$

The proof of Theorem 4 follows an approach inspired by Yan & Procaccia (2021), where the core allocation is approximated using sampled coalitions. The key idea is to leverage the properties of the VC-dimension of a function class to bound the probability of deviating from the true allocation in the core. To establish this result, we introduce the following two known lemmas, which play a crucial role in the proof.

Before proving the theorem, we first introduce a lemma regarding the VC-dimension of a function class, as this concept is essential to understanding the behavior of the classifier we employ in the proof.

**Lemma 10.** *Let  $\mathcal{F}$  be a function class from  $\mathcal{X}$  to  $\{-1, 1\}$ , and let  $\mathcal{G}$  have VC-dimension  $d$ . Then, with  $m = O\left(\frac{d + \log(\frac{1}{\Delta})}{\delta^2}\right)$  i.i.d. samples  $\{x^1, \dots, x^m\} \sim \mathcal{P}$ , we have:*

$$\left| \Pr_{x \sim \mathcal{P}}[f(x) \neq y(x)] - \frac{1}{m} \sum_{i=1}^m \mathbb{1}_{f(x^i) \neq y(x^i)} \right| \leq \delta,$$

for all  $f \in \mathcal{F}$  and with probability  $1 - \Delta$ .

This lemma essentially states that if the VC-dimension of a function class is  $d$ , then by taking a sufficient number of samples  $m$ , the empirical error rate of a classifier  $f$  on those samples is close to the true error rate with high probability (i.e.,  $1 - \Delta$ ).

In the context of the theorem, we use linear classifiers to represent the core allocation constraints. The following lemma establishes the VC-dimension of the class of linear classifiers we use.

**Lemma 11.** *The function class  $\mathcal{F}^n = \{x \mapsto \text{sign}(w \cdot x) : w \in \mathbb{R}^n\}$  has VC-dimension  $n$ .*

This lemma states that the VC-dimension of the class of linear classifiers is equal to the dimension  $n$  of the input space, which is important for bounding the number of samples required to approximate the core allocation effectively.

Now, we combine the insights from the previous lemmas to prove the theorem.

*Proof.* Consider a coalition  $C$  sampled from the distribution  $\mathcal{P}$ . We represent the coalition as a vector  $z^C = (z^C, -A_C(s, a_C), 1)$ , where  $z^C \in \{0, 1\}^n$  is the indicator vector for the coalition and  $A_C(s, a_C)$  is the total allocation for the agents not in  $C$ .

We define a linear classifier  $f$  based on parameters  $w^f = (A, 1, \epsilon)$ , where  $w^f \in \mathbb{R}^{n+2}$ . The classifier  $f(z^C) = \text{sign}(w^f \cdot z^C)$  is designed to capture the core allocation for each coalition  $C$ .

To ensure coalition rationality, we want the classifier  $f$  to satisfy  $f(z^C) = 1$  for all coalitions  $C \subseteq N$ . This ensures that the allocation is in the core for all coalitions. The class of such classifiers is:

$$\mathcal{F} = \{z \mapsto \text{sign}(w \cdot z) : w = (A, 1, \epsilon), A \in \mathbb{R}^n\}.$$

This class of functions  $\mathcal{F}$  has VC-dimension at most  $n + 2$  by Lemma 11.

Now, solving the quadratic programming problem on  $m$  samples of coalitions  $\{C_1, \dots, C_m\}$  provides a solution  $(\hat{A}, \hat{\epsilon})$ , and the corresponding classifier  $\hat{f}$ . For each sample coalition  $C_k$ , we have  $\hat{f}(z^{C_k}) = 1$ .

864 By applying Lemma 10, with probability  $1 - \Delta$ , we obtain the following inequality:  
 865

$$866 \quad 867 \quad \Pr_{C \sim \mathcal{P}} \left[ \sum_{i \in C} \hat{A}_i - A_C(s, a_C) + \hat{\epsilon} \geq 0 \right] \geq 1 - \delta. \\ 868$$

869 This shows that the allocation vector generated by solving the quadratic programming problem over  
 870 the sampled coalitions is within the  $\delta$ -probable core with high probability (i.e., with probability at  
 871 least  $1 - \Delta$ ). Thus, Theorem 4 is proved.  $\square$   
 872

### 873 A.7 TRUST-REGION DECOMPOSITION AND LOWER BOUNDS ON POLICY IMPROVEMENT

874 In this section, we discuss based on the definition  $A_C(s, a_C) = \mathbb{E}_{a_{N \setminus C} \sim \pi_{N \setminus C}}[Q(s, a_C, a_{N \setminus C})] -$   
 875  $V(s)$ , and derive Theorem 5 under the centralized TRPO/PPO framework. This section derives  
 876 theoretical lower bounds on the individual log-probability improvement  $\Delta \log \pi_i(a_i | s)$  when each  
 877 agent performs a policy update based on the allocated individual advantage  $A_i(s, a)$  for the given  
 878 sample  $(s, a)$ .  
 879

880 Under our setting, the joint policy factorizes as  $\pi(a | s) = \prod_{i \in N} \pi_i(a_i | s)$ . We aim to maximize  
 881 the local advantage improvement allocated to each agent while controlling the overall joint KL  
 882 divergence.  
 883

884 Given action  $a = (a_i, a_{-i})$ , consider the global policy-update problem:  
 885

$$886 \quad \max_{\{\pi'_i\}} \sum_{i \in N} \mathbb{E}_{a_i \sim \pi_i} [r_i(a_i | s) A_i(s, a)] \quad \text{s.t.} \quad \text{KL}(\pi'(\cdot | s) \| \pi(\cdot | s)) \leq \delta, \quad (20)$$

888 where  $r_i(a_i | s) = \pi'_i(a_i | s) / \pi_i(a_i | s)$ .  
 889

890 Due to factorization, the joint KL satisfies  
 891

$$892 \quad \text{KL}(\pi' \| \pi) = \sum_{i \in N} \text{KL}(\pi'_i \| \pi_i),$$

893 which implies that there is a single global trust-region constraint.  
 894

895 Relaxing the constraint with  $\eta > 0$  yields the penalized form:  
 896

$$897 \quad \max_{\{\pi'_i\}} \left( \sum_{i \in N} \mathbb{E}_{a_i \sim \pi_i} [r_i(a_i | s) A_i(s, a)] - \frac{1}{\eta} \sum_{i \in N} \text{KL}(\pi'_i \| \pi_i) \right). \quad (21)$$

898 The objective fully decomposes across  $\pi'_i$ , producing  $n$  independent subproblems:  
 899

$$900 \quad \max_{\pi'_i} \left( \mathbb{E}_{a_i \sim \pi_i} [r_i(a_i | s) A_i(s, a)] - \frac{1}{\eta} \text{KL}(\pi'_i \| \pi_i) \right), \quad \forall i. \quad (22)$$

901 Let  $q_i(a_i) = \pi'_i(a_i | s)$  and  $p_i(a_i) = \pi_i(a_i | s)$ . The subproblem becomes  
 902

$$903 \quad \max_{q_i} \sum_{a_i} q_i(a_i) A_i(s, a) - \frac{1}{\eta} \sum_{a_i} q_i(a_i) \log \frac{q_i(a_i)}{p_i(a_i)},$$

904 subject to  $\sum_{a_i} q_i(a_i) = 1$ .  
 905

906 Construct the Lagrangian  
 907

$$908 \quad \mathcal{L}(q_i, \lambda) = \sum_{a_i} q_i(a_i) A_i(s, a) - \frac{1}{\eta} \sum_{a_i} q_i(a_i) \log(q_i / p_i) + \lambda \left( \sum_{a_i} q_i - 1 \right).$$

909 Taking the derivative w.r.t.  $q_i(a_i)$  and setting it to zero yields  $\log(q_i / p_i) = \eta A_i(s, a) + c$ . Thus the  
 910 optimal update is  
 911

$$912 \quad \pi'_i(a_i | s) = \frac{\pi_i(a_i | s) \exp(\eta A_i(s, a))}{Z_i(s, a_{-i})}, \quad Z_i = \mathbb{E}_{a_i \sim \pi_i} [\exp(\eta A_i(s, a))], \quad (23)$$

918 and consequently

$$919 \quad \Delta \log \pi_i(a_i | s) = \eta A_i(s, a) - \log Z_i(s, a_{-i}).$$

920  
921 If  $m_i \leq A_i(s, a) \leq M_i$  (define  $R_i = M_i - m_i$ ), let  $X = A_i(s, a)$  with  $a_i \sim \pi_i$ . Hoeffding's lemma  
922 gives

$$923 \quad \log Z_i \leq \eta \mathbb{E}[X] + \frac{\eta^2 R_i^2}{8}.$$

924 Hence,

$$925 \quad \Delta \log \pi_i(a_i | s) \geq \eta(A_i(s, a) - \mathbb{E}_{a_i \sim \pi_i}[A_i(s, a)]) - \frac{\eta^2 R_i^2}{8}. \quad (24)$$

926 The CORA coalition constraint states that for any  $C \subseteq N$ ,

$$927 \quad \sum_{j \in C} A_j(s, a) \geq A_C(s, a_C) - \epsilon.$$

928 It can be proven that  $\mathbb{E}_{a_i \sim \pi_i}[A_i(s, a)] \leq \epsilon$ . For any given  $(s, a)$ , we have  $A_i(s, a) = A_N(s, a) -$   
929  $\sum_{j \neq i} A_j(s, a)$ . This can be rewritten as:  $A_i(s, a) \leq A_N(s, a) - A_{N-i}(s, a) + \epsilon$ . Since  $A_N =$   
930  $Q(s, a) - V(s)$ , and  $A_C(s, a) = Q_C(s, a) - V(s) = \mathbb{E}_{a_C \sim \pi_C}[Q(s, a)] - V(s)$ , we have:

$$931 \quad \mathbb{E}_{a_i \sim \pi_i}[A_i(s, a)] \leq \mathbb{E}_{a_i \sim \pi_i}[Q(s, a) - V(s)] - \mathbb{E}_{a_i \sim \pi_i}[Q_{N-i}(s, a_{N-i}) - V(s)] + \epsilon.$$

932 Since  $\mathbb{E}_{a_i \sim \pi_i}[Q(s, a)] = Q_{N-i}(s, a_{N-i})$ , and  $\mathbb{E}_{a_i \sim \pi_i}[Q_{N-i}(s, a)] = Q_{N-i}(s, a_{N-i})$ , it follows  
933 that:

$$934 \quad \mathbb{E}_{a_i \sim \pi_i}[A_i(s, a)] \leq 0 + \epsilon.$$

935 Thus the final lower bound on the individual log-probability improvement becomes

$$936 \quad \Delta \log \pi_i(a_i | s) \geq \eta(A_i(s, a) - \epsilon) - \frac{\eta^2 R_i^2}{8}. \quad (25)$$

937 The coalition log-probability change is  $\Delta \log \pi_C(a_C | s) = \sum_{i \in C} \Delta \log \pi_i(a_i | s)$ . Thus,

$$938 \quad \Delta \log \pi_C(a_C | s) \geq \eta \left( \sum_{i \in C} A_i(s, a) - |C| \epsilon \right) - \sum_{i \in C} \frac{\eta^2 R_i^2}{8}. \quad (26)$$

939 Applying the coalition advantage constraint  $\sum_{i \in C} A_i \geq A_C(s, a_C) - \epsilon$  gives a tighter lower bound:

$$940 \quad \Delta \log \pi_C(a_C | s) \geq \eta(A_C(s, a_C) - (1 + |C|) \epsilon) - \sum_{i \in C} \frac{\eta^2 R_i^2}{8}. \quad (27)$$

941 Thus, we can derive Theorem 5.

942 If  $A_C(s, a) \geq A_N(s, a) \geq 0$ , then  $\sum_{i \in C} A_i \geq A_C(s, a) - \epsilon \geq A_N(s, a) - \epsilon$ , and

$$943 \quad \sum_{i \notin C} A_i(s, a) = A_N(s, a) - \sum_{i \in C} A_i(s, a) \leq \epsilon.$$

944 Thus a high-value coalition  $C$  receives almost all advantage  $A_N(s, a) - \epsilon$ .

945 If  $A_C(s, a) \geq 0 > A_N(s, a)$ , then  $\sum_{i \in C} A_i \geq A_C(s, a) - \epsilon \geq -\epsilon$ , and

$$946 \quad \sum_{i \notin C} A_i(s, a) = A_N(s, a) - \sum_{i \in C} A_i(s, a) \leq A_N(s, a) + \epsilon.$$

947 Minimizing  $\epsilon$  assigns the coalition  $C$  only small cost  $-\epsilon$ , while  $N \setminus C$  absorbs the larger cost  
948  $A_N(s, a) + \epsilon$ . Thus, even when the global action fails but  $A_C(s, a)$  is valuable, the coalition's action  
949 probability is preserved—this mechanism is the core driving principle of CORA.

972  
973  
974**Algorithm 1** Core Advantage Decomposition (CORA)

---

1: **Initialize:** Central critic network  $\theta_V, \theta_Q$ ; actor network  $\phi_i$  for each agent  $i$   
2: **for** each training episode  $e = 1, \dots, E$  **do**  
3:   Initialize state  $s^0$  and experience buffer  
4:   **for** each step  $t$  **do**  
5:     Sample action  $a_i^t$  from  $\pi_i(a_i|s^t; \phi_i)$  for each agent  
6:     Execute the joint action  $(a_1^t, \dots, a_n^t)$   
7:     Get reward  $r^{t+1}$  and next state  $s^{t+1}$   
8:     Add data to experience buffer  
9:   **end for**  
10:   Collate episodes in buffer into a single batch  
11:   Compute the target value:  $y^t = r(s^t, a^t) + \gamma Q(s^{t+1}; \theta_V)$   
12:   **for**  $t = 1, \dots, T$  **do**  
13:     Sample  $m$  coalitions  $\mathcal{C} = \{C_1, \dots, C_m\} \subseteq 2^N$   
14:     **for** each coalition  $C \in \mathcal{C}$  **do**  
15:       Estimate coalitional advantage  $A_C(s^t, a_C^t)$  for each coalition  $C \in \mathcal{C}$ .  
16:       where  $\bar{a}_i = \arg \max_{a_i} \pi_i(a_i|s_i^t; \phi_i)$   
17:     **end for**  
18:     Estimate grand coalition  $N$ 's advantage  $A(s^t, a^t)$  with GAE estimator  
19:     Solve the programming problem to obtain credit allocation  $\hat{A}_i^t$   
20:   **end for**  
21:   Update actor networks  $\phi_i$  using PPO-clipped policy gradient:  
22:     
$$\nabla_{\phi_i} \log \pi_{\phi_i}(a_i^t|s_i^t) \cdot \text{clip} \left( \frac{\pi_{\phi_i}(a_i^t|s_i^t)}{\pi_{\phi_i}^{\text{old}}(a_i^t|s_i^t)}, 1 - \epsilon, 1 + \epsilon \right) \cdot \hat{A}_i^t$$
  
23:     Update critic  $\theta_V$  using TD error:  $\sum_t (V(s^t; \theta_V) - y^t)^2$   
24:     Update critic  $\theta_Q$  using error:  $\sum_t (Q(s^t, a^t; \theta_Q) - y^t)^2$   
**end for**


---

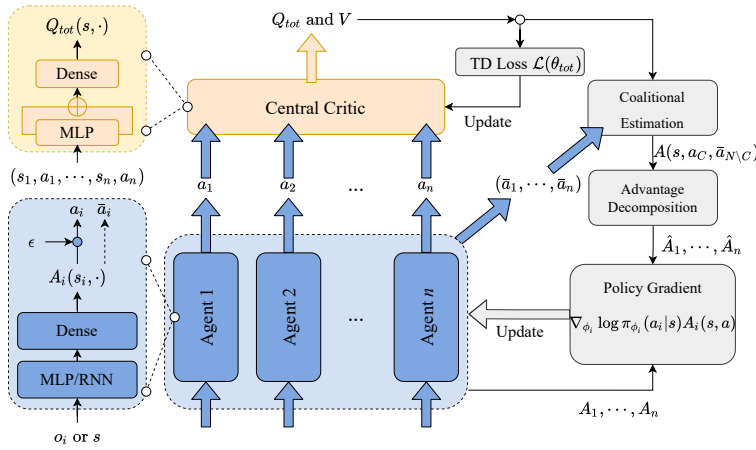
1001  
1002  
1003  
1004  
1005  
1006  
1007  
1008  
1009  
1010  
1011  
1012  
1013  
1014  
1015  
1016  
1017  
1018  
1019  
1020  
1021  
1022  
1023  
1024  
1025


Figure 7: The framework of CORA in Multi-Agent Reinforcement Learning.

1026  
1027

## A.8 ALGORITHM PSEUDOCODE AND DIAGRAM

1028  
1029  
1030  
1031  
1032

Algorithm 1 outline the implementation of CORA within a standard actor–critic training loop. At each update, a set of coalitions is sampled, and the corresponding coalitional advantages are estimated. A constrained quadratic program is then solved to assign individual credits, which are used to guide policy updates. This procedure ensures that policy gradients reflect coalition-level contributions, encouraging coalitional coordination.

1033  
1034  
1035

As illustrated in Figure 7, the framework demonstrates the process of Coalitional Advantage Estimation and subsequent Credit Allocation in policy gradient methods.

1036  
1037  
1038

## A.9 EXPERIMENTAL DETAILS

1039  
1040  
1041  
1042  
1043  
1044  
1045  
1046  
1047

Table 1: Training Hyperparameters for Each Environment

Environment	Actor LR	Critic LR	$\gamma$	GAE $\lambda$	Clip $\epsilon$	Parallel Envs
Matrix Games	$5 \times 10^{-4}$	$5 \times 10^{-3}$	0.99	0.95	0.3	4
Differential Games	$5 \times 10^{-5}$	$5 \times 10^{-4}$	0.99	0.95	0.2	4
Multi-Agent MuJoCo	$5 \times 10^{-4}$	$5 \times 10^{-3}$	0.99	0.95	0.2	4
VMAS (Navigation)	$5 \times 10^{-4}$	$5 \times 10^{-3}$	0.99	0.95	0.2	64
VMAS (Others)	$5 \times 10^{-4}$	$5 \times 10^{-3}$	0.99	0.95	0.2	16

1048  
1049  
1050  
1051  
1052  
1053  
1054

All experiments were conducted on platforms with AMD 7970X 32-Core CPU, 128GB RAM, and RTX 4090 GPU (24GB). Each algorithm was trained with a two-layer multilayer perceptron (MLP) with a hidden width of 64, except for the *Give-Way* scenario in VMAS, which used a custom network structure. Unless otherwise specified, each configuration was run five times with different random seeds for both the algorithm and the environment. We used the full coalition set ( $2^n$  coalitions) for credit assignment across all tasks. For efficiency, 64 parallel environments were used in the *Navigation* task of VMAS, while others used 16 or 4 as listed.

1055  
1056  
1057  
1058  
1059  
1060  
1061

## A.10 ABLATION STUDY OF COALITION SAMPLE SIZE, STD TERM

To evaluate the impact of coalition sampling size on performance, we conduct an ablation experiment in a differential game environment with 5 agents. Due to the high computational cost in large-scale multi-agent tasks, this experiment focuses on the 5D differential game setting, which balances complexity and tractability.

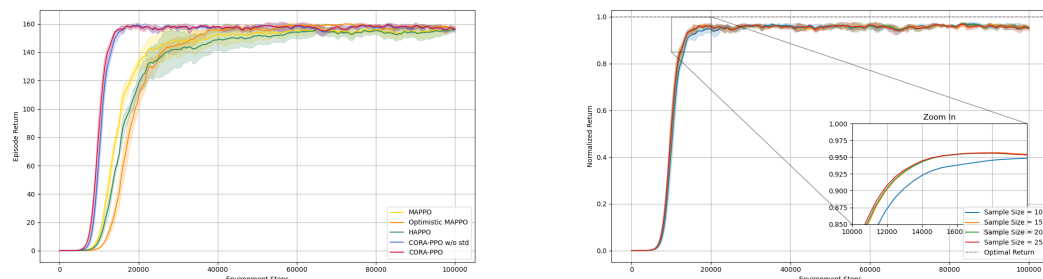
1072  
1073  
1074  
1075  
1076  
1077

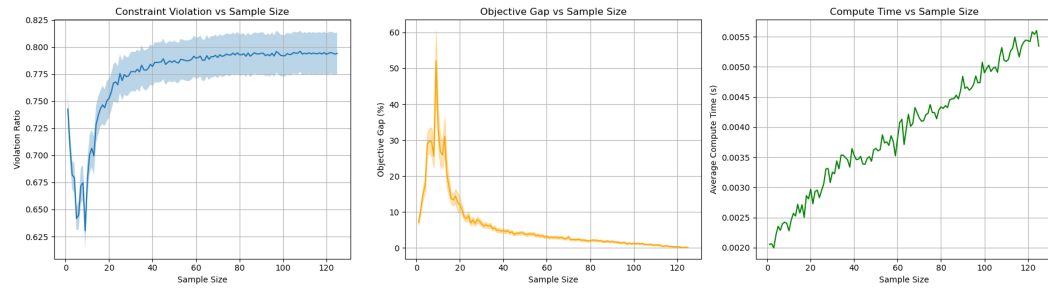
Figure 8: Training performance in the 5D differential game scenario. **Left:** Comparison among baseline methods. **Right:** Effect of coalition sampling size (sample sizes = 10, 15, 20, 25; full coalition size is  $2^n - 2 = 30$ ). All algorithms are repeated 5 times to obtain a 95% confidence interval. Key hyperparameters: Actor learning rate  $5 \times 10^{-5}$ , Critic learning rate  $5 \times 10^{-4}$ ,  $\gamma = 0.99$ , GAE  $\lambda = 0.95$ , 10 epochs per update, clip  $\epsilon = 0.2$ , and 4 parallel environments.

1078  
1079

As shown in Figure 8, increasing the coalition sample size generally improves performance, particularly in the early stages of training, as highlighted in the zoomed-in window. However, even with smaller sampling sizes (e.g., 10 or 15), the CORA algorithm still achieves competitive results. This

1080 indicates that CORA is robust to sample efficiency and remains effective under reduced computation,  
 1081 making it applicable to environments with a moderate number of agents. In addition, CORA  
 1082 with variance often improves performance.

1083 The original credit allocation formulation is a constrained quadratic program, which we relax by  
 1084 linearizing the variance term, resulting in a more efficient linear programming form.  
 1085



1096  
 1097 Figure 9: Error and Time Cost of Approximate Credit Assignment. Violation Ratio: proportion of  
 1098 coalition rationality constraints that are violated; Objective Gap: percentage difference in optimiza-  
 1099 tion objective compared to the full solution; Compute Time: average runtime across trials. (Number  
 1100 of agents = 7; Advantage functions are randomly generated across 20 trials.)  
 1101

1102 Figure 9 shows that using only a small number of sampled coalitions yields an accurate and com-  
 1103putationally efficient approximation. While constraint satisfaction may degrade slightly with fewer  
 1104 samples, the overall objective gap remains low, and compute time is significantly reduced. This  
 1105 supports the use of approximate credit assignment methods in large-scale scenarios, where full enu-  
 1106 meration of  $2^n$  coalitions is infeasible.  
 1107

## B LLM USAGE

1110 We used a large language model (LLM) as an assistive tool for: (i) language editing (grammar and  
 1111 clarity), (ii) consistency checks on LaTeX labels and formatting. The LLM did not generate research  
 1112 ideas, proofs and experimental results. No proprietary or non-anonymized data were provided to the  
 1113 LLM.  
 1114  
 1115  
 1116  
 1117  
 1118  
 1119  
 1120  
 1121  
 1122  
 1123  
 1124  
 1125  
 1126  
 1127  
 1128  
 1129  
 1130  
 1131  
 1132  
 1133